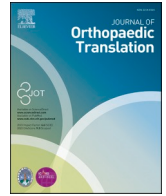




Contents lists available at ScienceDirect

Journal of Orthopaedic Translation

journal homepage: www.journals.elsevier.com/journal-of-orthopaedic-translation

IRF1 governs the expression of SMARCC1 via the GCN5-SETD2 axis and actively engages in the advancement of osteoarthritis

Dong Wang^{a,b,c,e,1}, Yujun Zhang^{a,1}, Liangping Zhang^{a,1}, Du He^a, Lan Zhao^a, Zhimin Miao^a, Wei Cheng^{a,b}, Chengyue Zhu^{a,b,c}, Li Zhu^a, Wei Zhang^{a,b}, Hongting Jin^{a,d,*}, Hang Zhu^{a,**}, Hao Pan^{a,b,c,***}

^a Department of Orthopaedics, Hangzhou TCM Hospital Affiliated to Zhejiang Chinese Medical University (Hangzhou Hospital of Traditional Chinese Medicine), Hangzhou 310000, Zhejiang Province, PR China

^b Department of Orthopaedics, Hangzhou Dingqiao Hospital, Huanding Road NO 1630, Hangzhou 310021, Zhejiang Province, PR China

^c Institute of Orthopaedics and Traumatology, Hangzhou Traditional Chinese Medicine Hospital Affiliated to Zhejiang Chinese Medical University, Tiyuchang Road NO 453, Hangzhou 310007, Zhejiang Province, PR China

^d Institute of Orthopaedics and Traumatology, The First Affiliated Hospital of Zhejiang Chinese Medical University, Hangzhou, PR China

^e Hangzhou Lin'an District Traditional Chinese Medicine Hospital, Hangzhou, PR China

ARTICLE INFO

Keywords:

Epigenetics
GCN5
IRF1-SMARCC1 axis
Macrophages
Osteoarthritis
SETD2

ABSTRACT

Background: Osteoarthritis (OA) is a degenerative joint disease characterized by the breakdown of joint cartilage and underlying bone. Macrophages are a type of white blood cell that plays a critical role in the immune system and can be found in various tissues, including joints. Research on the relationship between OA and macrophages is essential to understand the mechanisms underlying the development and progression of OA.

Objective: This study was performed to analyze the functions of the IRF1-GCN5-SETD2-SMARCC1 axis in osteoarthritis (OA) development.

Methods: A single-cell RNA sequencing (scRNA-seq) dataset, was subjected to a comprehensive analysis aiming to identify potential regulators implicated in the progression of osteoarthritis (OA). In order to investigate the role of IRF1 and SMARCC1, knockdown experiments were conducted in both OA-induced rats and interleukin (IL)-1 β -stimulated chondrocytes, followed by the assessment of OA-like symptoms, secretion of inflammatory cytokines, and polarization of macrophages. Furthermore, the study delved into the identification of aberrant epigenetic modifications and functional enzymes responsible for the regulation of SMARCC1 by IRF1. To evaluate the clinical significance of the factors under scrutiny, a cohort comprising 13 patients diagnosed with OA and 7 fracture patients without OA was included in the analysis.

Results: IRF1 was found to exert regulatory control over the expression of SMARCC1, thus playing a significant role in the development of osteoarthritis (OA). The knockdown of either IRF1 or SMARCC1 disrupted the pro-inflammatory effects induced by IL-1 β in chondrocytes, leading to a mitigation of OA-like symptoms, including inflammatory infiltration, cartilage degradation, and tissue injury, in rat models. Additionally, this intervention resulted in a reduction in the predominance of M1 macrophages both in vitro and in vivo. Significant epigenetic modifications, such as abundant H3K27ac and H3K4me3 marks, were observed near the SMARCC1 promoter and 10 kb upstream region. These modifications were attributed to the recruitment of GCN5 and SETD2, which are functional enzymes responsible for these modifications. Remarkably, the overexpression of either GCN5 or SETD2 restored SMARCC1 expression in rat cartilages or chondrocytes, consequently exacerbating the OA-like symptoms.

* Corresponding author. Institute of Orthopaedics and Traumatology, The First Affiliated Hospital of Zhejiang Chinese Medical University, Hangzhou, PR China.

** Corresponding author. Department of Orthopaedics, Hangzhou TCM Hospital Affiliated to Zhejiang Chinese Medical University Hangzhou 310000, Zhejiang Province, PR China.

*** Corresponding author. Hao Pan: Department of Orthopaedics, Hangzhou TCM Hospital Affiliated to Zhejiang Chinese Medical University Hangzhou 310000, Zhejiang Province, PR China.

E-mail addresses: hongtingjin@163.com (H. Jin), 13958015488@163.com (H. Zhu), harper1966@alu.zcmu.edu.cn (H. Pan).

¹ These author contributed equally to this work.

<https://doi.org/10.1016/j.jot.2024.01.002>

Received 6 July 2023; Received in revised form 13 October 2023; Accepted 13 January 2024

2214-031X/© 2024 The Authors. Published by Elsevier B.V. on behalf of Chinese Speaking Orthopaedic Society. This is an open access article under the CC BY-NC-ND license (<http://creativecommons.org/licenses/by-nc-nd/4.0/>).

Conclusion: This research postulates that the transcriptional activity of SMARCC1 can be influenced by IRF1 through the recruitment of GCN5 and SETD2, consequently regulating the H3K27ac and H3K4me3 modifications in close proximity to the SMARCC1 promoter and 10 kb upstream region. These modifications, in turn, facilitate the M1 skewing of macrophages and contribute to the progression of osteoarthritis (OA).

The Translational Potential of this Article: The study demonstrated that the regulation of SMARCC1 by IRF1 plays a crucial role in the development of OA. Knocking down either IRF1 or SMARCC1 disrupted the pro-inflammatory effects induced by IL-1 β in chondrocytes, leading to a mitigation of OA-like symptoms in rat models. These symptoms included inflammatory infiltration, cartilage degradation, and tissue injury. These findings suggest that targeting the IRF1-SMARCC1 regulatory axis, as well as the associated epigenetic modifications, could potentially be a novel approach in the development of OA therapies, offering new opportunities for disease management and improved patient outcomes.

Abbreviation list

Abbr	Full name		
IRF1	Interferon Regulatory Factor 1	CD206	Cluster of Differentiation 206
SMARCC1	SWI/SNF Related, Matrix Associated, Actin Dependent Regulator of Chromatin	THP-1	Acute Monocytic Leukemia Cell Line
C1	Subfamily C, Member 1	TUNEL	Terminal Deoxynucleotidyl Transferase dUTP Nick End Labeling
GCN5	General Control of Amino Acid Synthesis Protein 5	IHC	Immunohistochemistry
SETD2	SET Domain Containing 2	WB	Western Blot
OA	Osteoarthritis	ELISA	Enzyme-Linked Immunosorbent Assay
RNA	Ribonucleic Acid	H3K27ac	Histone 3 Lysine 27 Acetylation
qPCR	Quantitative Polymerase Chain Reaction	TNF- α	Tumor Necrosis Factor Alpha
FBS	Fetal Bovine Serum	IL-12	Interleukin 12
CD86	Cluster of Differentiation 86	IL-10	Interleukin 10
		MCP-1	Monocyte Chemoattractant Protein 1
		TGF- β	Transforming Growth Factor Beta
		ANOVA	Analysis of Variance

1. Introduction

Osteoarthritis (OA) is a progressive joint disorder characterized primarily by the erosion of articular cartilage, remodeling of subchondral bone, synovial inflammation, and the formation of osteophytes [1,2]. Osteoarthritis (OA) is the prevailing type of arthritis and commonly affects the knees, hands, hips, and other joints in the appendicular skeleton [3]. The prevalence of osteoarthritis (OA) continues to rise, impacting approximately 7% of the global population. It is estimated that over 500 million individuals worldwide are affected by this condition [4]. The precise etiology of osteoarthritis (OA) remains elusive; however, several risk factors have been identified, including advanced age, obesity, genetic predisposition, traumatic injury, and other underlying joint pathologies [5]. Common clinical symptoms for patients include joint pain, stiffness, and decreased mobility, which significantly affects the quality of life of the bearing individuals [6].

It has been clear that the chronic inflammation is the major culprit leading to the degradation of cartilage and bone [7,8]. Inflammation is controlled by a myriad of immune cells. Tissue-macrophages are phagocytic cells that are virtually present in almost every tissue including brain, skin, liver, and joints with the primary roles in maintaining tissue homeostasis and protecting against infection [9]. They can be roughly allocated into the “classically activated” (M1) phenotype with antimicrobial and pro-inflammatory properties, or the “alternatively activated” (M2) phenotype with anti-inflammatory and pro-resolving capacities [9]. An imbalance between M1 and M2 type macrophages, oftentimes a predominance of M1 type, is closely linked to the chronic inflammation in progression of a multitude of diseases, including OA [10].

Through the analysis of the single-cell RNA sequencing (scRNA-seq) dataset GSE152805, which includes transcriptome data from three pairs of cartilage tissues and synovium, and subsequent integrated bioinformatics analyses, two key molecules, namely interferon regulatory factor

1 (IRF1) and SWI/SNF related, matrix associated, actin dependent regulator of chromatin subfamily c member 1 (SMARCC1), were identified. These molecules exhibited high expression levels in osteoarthritis (OA) chondrocytes and were found to be associated with the inflammatory activation of macrophages. IRF1, as the founding member of the interferon regulatory factor (IRF) family of transcription factors, plays a critical role in various biological processes. This includes immune response modulation, induction of anti-viral cytokines such as interferons, regulation of cell growth, and apoptosis [11]. IRF1 is activated by a variety of stimuli such as DNA damage [12] and interferons [13]. IRF1 orchestrates several antimicrobial activities and controls the expression of inducible nitric oxide synthase (iNOS) and guanylate binding proteins that are implicated in multiple inflammatory diseases [14]. While it plays a protective role in innate immunity-related inflammatory conditions, IRF1 is oftentimes pathogenic in chronic inflammatory diseases [15]. Interestingly, IRF1 has been associated with the M1 skewing of macrophages [16], which indicates that it possibly induces M1 macrophage accumulation during OA pathogenesis. SMARCC1 is a core subunit of the SWI/SNF complex that functions by interfering with histone-DNA contacts using energy from ATP [17]. Meanwhile, SMARCC1 also regulates the post-transcriptional stabilization of other major components of the SWI/SNF complex, such as SNF5, BRG1, and BAF60a [18]. The SMARCC1-containing SWI/SNF complexes have reportedly linked to activation and proliferation of T cells [19]. Moreover, SMARCC1 has been reported to promote the Th2 type immune response and induce M2 polarization of macrophages, leading to exacerbated atopic dermatitis [20].

Despite its well-established role in various biological processes, the specific involvement of IRF1 in macrophage polarization during the progression of osteoarthritis (OA) remains poorly understood. In light of this knowledge gap, our study aimed to explore the possibility that IRF1 acts as a regulatory factor for SMARCC1, thus playing a crucial role in orchestrating macrophage polarization. The primary objective of this research was to investigate the roles of IRF1 and SMARCC1 in the inflammatory response observed in OA. Furthermore, our study aimed to

unravel the underlying molecular mechanisms that govern these processes. By conducting a comprehensive investigation, we sought to shed light on the intricate interplay between these molecules and their contributions to OA-related inflammation.

2. Materials and methods

2.1. Clinical sample collection

The research participants comprised 13 patients who were diagnosed with osteoarthritis (OA) and had undergone total knee replacement at Hangzhou TCM Hospital, which is affiliated with Zhejiang Chinese Medical University. The cartilage samples obtained from the medial femoral condyle of these osteoarthritis patients were categorized as the OA group. Furthermore, the study incorporated a control group consisting of articular cartilage samples collected from 7 patients who underwent total hip replacement as a result of a femoral neck fracture. These particular samples served as the normal control group.

2.2. Bioinformatics

scRNA-seq dataset GSE152805 which contains single-cell transcriptome data of three pairs of cartilage tissues and synovium was downloaded from GEO database and analyzed. The "Seurat" R package was used for quality control. The data were standardized using the logNormalize method and integrated by canonical correspondence analysis (CCA). downloaded the GEO dataset GSE112655 that contains the ChIP-seq data of H3K27ac, H3K36me3, H3K4me1, H3K4me3, and H3K9me3 from 11 OA patients. The ChIP-seq data was analyzed using MACS2 for peak calling. Subsequently, IGV was employed to visualize the ChIP-seq data.

2.3. Reverse transcription quantitative polymerase chain reaction (RT-qPCR)

The intracellular RNA was isolated from chondrocytes and tissues utilizing the RNeasy Plus Mini kit (Tsingke Biotechnology Co., Ltd., China). The evaluation of RNA expression was conducted using the 2- $\Delta\Delta$ CT method, with GAPDH employed as an internal reference. The primers used are listed in Table 1.

2.4. Rat chondrocyte collection and treatment

The experimental procedures involving animals in this study were approved by the Institutional Animal Care and Use Committee of the Animal Experiment Center at Zhejiang Chinese Medical University.

Sprague–Dawley (SD) rats obtained from Hangzhou Qizhen Laboratory Animal Technology Co., Ltd., Zhejiang, China, were employed for the study. The rats were in a healthy growth state but were euthanized using an excessive dose of pentobarbital sodium. Under sterile conditions, the fibrous connective tissue was carefully removed, and the cartilage samples were then cut into 1-mm cubes. To ensure sterility, the tissue was thoroughly washed multiple times using phosphate-buffered saline (PBS) supplemented with sodium penicillin and gentamicin. After the washing steps, a 0.25 % trypsin solution was added at a ratio of 1:5, and the tissue was allowed to undergo digestion for 30 min. Subsequently, a 0.2 % type II collagenase solution was added at a ratio of 1:5, and the tissue was digested for a period of 16 h. The resulting cell suspension was collected after centrifugation and filtered through a 200-mesh filter at 1000 r/min for 5 min, with the supernatant being discarded. The cells, specifically chondrocytes, were then cultured in complete medium (Thermo Fisher Scientific, Rockford, IL, USA) supplemented with 10 % fetal bovine serum (FBS) and incubated at 37 °C with 5 % CO₂. Cells at passages 2 to 4 were utilized for subsequent experiments. To induce an in vitro osteoarthritis (OA)-like condition, the chondrocytes were treated with interleukin (IL)-1 β at a concentration of 10 ng/mL for further experimentation.

2.5. Chromatin immunoprecipitation (ChIP)-qPCR

To examine the binding of IRF1, GCN5, and SETD2 to the SMARCC1 promoter and its upstream region, the EZ-ChIP kit (Millipore, USA) was utilized. Initially, the cells were treated with 1 % formaldehyde for 10 min to crosslink the proteins and DNA. Following this, the cells were lysed using SDS lysis buffer, and DNA fragmentation was accomplished through ultrasonication. The resulting lysates were subjected to overnight immunoprecipitation at 4 °C using specific antibodies, including IgG (1:300, ab99757, Abcam, UK), H3K4me3 (#MA5-11199, Thermo Fisher Scientific), H3K27ac (#MA5-23516, Thermo Fisher Scientific), IRF1 (ab232861, Abcam), SETD2 (#PA5-102710, Thermo Fisher Scientific), and GCN5 (#PA5-86489, Thermo Fisher Scientific). After the immunoprecipitation, the antibody–chromatin complexes were precipitated using protein G agarose at 4 °C for 1 h. Subsequently, the complexes underwent a series of washes, and the DNA was eluted. The protein-DNA complexes were then de-crosslinked, and the DNA was collected and purified for subsequent analysis using quantitative PCR (qPCR).

2.6. Immunofluorescence staining

Healthy chondrocytes were treated with a permeabilization solution and incubated at room temperature for 20 min. Subsequently, a closure buffer, diluted at a ratio of 1:100, was added to the chondrocytes and placed in a humidified chamber at 37 °C for 30 min. Following this, CD86 (#MA1-10293, Thermo Fisher Scientific) and CD206 (#PA5-114370, Thermo Fisher Scientific), both diluted at a ratio of 1:100, were introduced to the chondrocytes and incubated at 37 °C for 3 h. After the incubation, biotinylated goat anti-mouse IgG, diluted at a ratio of 1:100, was applied and incubated at 37 °C for 45 min. To stain the cell nuclei, DAPI was used, and the chondrocytes were examined under an inverted microscope.

2.7. Co-culture system

THP-1 monocytes were cultured in RPMI 1640 medium supplemented with 1 % antibiotics and 5 % fetal bovine serum (FBS). To induce the differentiation of THP-1 monocytes into M0 macrophages, the cells were treated with 50 ng/mL of 12-myristate 13-acetate (PMA) and incubated for 24 h. For the co-culture experiments, THP-1 cells at a concentration of 106 cells/mL were seeded into the upper chamber of a 24-well Transwell plate, while chondrocytes were seeded into the lower chambers at a concentration of 105 cells/mL. The cells were co-cultured

Table 1
Primers.

ID	Sequence(5'-3')
MMP3-F	CTGGACTCCGACACTCTGGA
MMP3-R	CAGGAAAGGTTCTGAAGTGACC
MMP13-F	TTGCAGAGCGCTACCTGAGATCAT
MMP13-R	TT TGCCAGTCACTCTA AGCCGAA
COL II-F	GGTGGAGCAGCAAGAGCAA
COL II-R	AGTGGACAGTAGACGGAGGAAA
iNOS-F	CTGGCAAGCCCAAGGTCTAT
iNOS-R	GGAGGCTCCGATCAATCCAG
COX-2-F	ATCATAAGCGAGGGCCAGCT
COX-2-R	AAGCGCAGTTTACGCTGTC
TNF- α -F	CATCCGTTCTCTACCCAGCC
TNF- α -R	AATTCTGAGCCCGAGTTGG
IL-6-F	CCCACCCTCCAACAAGATT
IL-6-R	GCTCCAGAGCAGAATGACCTA
Arg1-F	TCATCTGGGTGGATGCTCACAC
Arg1-R	GAGAATCTGGCACATCGGGAA
GAPDH-F	TGGTCACCGGGCTGCTT
GAPDH-R	AGCTTCCCGTTCTCAGCC

for 24 h and subsequently collected for further assays. To analyze the presence of CD86- or CD206-positive macrophages, flow cytometry was utilized as the detection method.

2.8. Cell counting kit-8 (CCK-8) method

Chondrocytes were cultured on 96-well cell culture plates at 5×10^3 cells per well. After 72 h, the CCK-8 solution (Thermo Fisher Scientific) was added to the medium at a ratio of 10 mL/100 mL for 4 h of incubation at 37 °C. Optical density (OD) was detected at 450 nm using an iMark microplate reader (Bio-Rad, USA), and the cell viability was calculated by reference to a standard curve.

2.9. 5-Ethynyl-2'-deoxyuridine (EdU) labeling assay

To analyze the proliferation of chondrocytes, the EdU-Apollo 567 in vitro kit (RiboBio Co., Ltd, Guangdong, China) was employed. Briefly, the cells were seeded in 96-well plates at a density of 1×10^4 cells per well. After 48 h, the cells were incubated with 50 μ M EdU labeling reagent for 2 h. Subsequently, the cells were fixed with 4 % polyformaldehyde, permeabilized with 0.5 % Triton X-100/PBS, and stained with Apollo reagent and DAPI.

3. Animals

A total of 35 juvenile Sprague–Dawley (SD) rats, aged two months, were housed in a specific pathogen-free (SPF) facility with controlled environmental conditions, including regulated temperature, humidity, and a 12-h alternating light–dark cycle. The rats were provided ad libitum access to SPF-grade feed and water. To induce osteoarthritis (OA), surgical excision of the anterior cruciate ligament (ACL) and medial meniscus was performed on the rats after intraperitoneal anesthesia using a 1 % pentobarbital sodium solution (40 mg/kg). A medial incision was made in the right hind knee, the joint capsule was incised, and the ACL was severed using scissors. The joint capsule and skin were then sutured. The rats' physical well-being and behavior were monitored daily throughout the study. Recombinant lentiviral vectors containing short hairpin RNA (shRNA) targeting the genes IRF1 and SMARCC1 were obtained from Genechem Co., Ltd. (Shanghai, China). Each rat with OA received intra-articular injections of 100 μ L saline solution combined with the corresponding lentiviral vectors (1×10^9 PFU). The injections were administered once every 5 days, starting one week after the initial surgery. After a 6-week treatment period, the rats were euthanized with an overdose of pentobarbital sodium. Both synovial fluid and intact joints were extracted for subsequent experimental analysis.

3.1. Safranin O staining

The intact rat joints were fixed in a 4 % paraformaldehyde solution, followed by paraffin embedding and sectioning at a thickness of 5 μ m using a microtome. The sections underwent dewaxing and hydration procedures, and then they were stained with hematoxylin for 10 s. After rinsing, the sections were stained with a 0.1 % fast green solution for 5 min and briefly immersed in glacial acetic acid for 5 s. Subsequently, the sections were incubated in a 0.5 % saffron O dye solution (provided by Takara Biotechnology Ltd., Liaoning, China) for 5 min. After drying at room temperature, the sections were made transparent by treating them with xylene for 5 min. They were then examined for tissue damage using a light microscope (Carl Zeiss, Oberkochen, Germany). Prior to examination, the sections were sealed with a neutral gel. The degree of tissue injury was assessed according to Mankin's scoring system [21].

3.2. Terminal deoxynucleotidyl transferase (TdT)-mediated dUTP nick end labeling (TUNEL)

The TUNEL kit (Roche Ltd, Basel, Switzerland) was used to examine apoptotic bodies in the 5- μ m cartilage tissue sections or isolated rat chondrocytes, following the instruction manual. The labeling was observed under a light microscope, and the rate of TUNEL-positive cells was calculated.

3.3. Western blot (WB) analysis

Total protein was extracted from cells using ice-cold RIPA buffer (Solarbio Science & Technology Co., Ltd., Beijing, China), and the protein concentration was determined using a bicinchoninic acid kit (Sigma–Aldrich, Merck KGaA, Darmstadt, Germany). An equal volume of the protein sample was separated by SDS-PAGE and transferred to a polyvinylidene fluoride membrane. The membrane was then blocked with 5 % non-fat milk. Subsequently, the membrane was probed with primary antibodies against IRF1 (ab232861, Abcam), SMARCC1 (#PA5-55058), Aggrecan (MA3-16888), Arg1 (ab96183, Abcam), iNOS (ab178945, Abcam), Collagen II (MA5-12789, Thermo Fisher Scientific), MMP13 (#PA5-27242, Thermo Fisher Scientific), and GAPDH (ab8245, Abcam) overnight at 4 °C. Afterward, the membrane was incubated with the secondary antibody (1:3,000, ab205718, Abcam) at room temperature for 1 h. The protein bands were visualized using enhanced chemiluminescence (ECL) reagent (GE Healthcare, Bucks, UK) and quantified using Image J.

3.4. Enzyme-linked immunosorbent assay (ELISA)

The synovial fluid of rats or the cell culture supernatant was centrifuged at 3000 r/min, and the concentrations of tumor necrosis factor-alpha (TNF- α), IL-6, IL-10, IL-12, macrophage cationic peptide 1 (MCP-1), transforming growth factor-beta (TGF- β), and IL-23 were analyzed using specific ELISA kits. The rat TNF- α (RTA00/DTA00D), rat IL-6 (R600B/D6050), rat IL-12 (D1200), IL-10 (D100B), MCP-1 (DY3144-05), TGF- β (DB100C), and IL-23 (D2300B) ELISA kits from Elabscience Biotechnology Co., Ltd. (Hubei, China) were used following the manufacturer's instructions. The optical density (OD) value at 450 nm was measured using an iMark microplate reader (Bio-Rad Laboratories, Hercules, CA, USA), and the concentrations of the inflammatory cytokines were determined by referring to the standard curve provided by the respective ELISA kits.

3.5. Immunohistochemistry (IHC)

The paraffin-embedded cartilage tissues were subjected to dewaxing and hydration processes. They were then treated with 3 % H₂O₂ and blocked with 5 % normal goat serum. Next, the sections were incubated overnight at 4 °C with primary antibodies against iNOS (ab178945, Abcam) and Arg1 (ab96183, Abcam). Following this, the sections were incubated with the secondary antibody (1:500, ab199091, Abcam) at 37 °C for 15 min. Subsequently, the sections were incubated with horseradish-labeled streptavidin working solution at 37 °C for 15 min. After color development using DAB and counter-staining with hematoxylin, the sections were dehydrated and sealed for microscopic analysis. Five non-overlapping fields of view were included in the analysis. Cells exhibiting brownish-yellow or brownish-brown granules in the nucleus were considered positive cells.

3.6. Hematoxylin and eosin (HE) staining

Tissue injury and inflammatory cell infiltration were assessed in the tissue sections obtained from paraffin-embedded cartilage samples. The 5- μ m sections were stained with hematoxylin solution (Solarbio) for 4 min, followed by rinsing. Subsequently, the sections were stained with

eosin solution (Solarbio) for 2 min. After the staining procedure, the tissue sections were fixed and sealed with neutral balsam for microscopic analysis.

3.7. Toluidine blue staining

The de-paraffinized sections were treated with a 0.5 % solution of high iodine acid for 10 min, followed by washing in running water for 5 min. Subsequently, the sections were incubated with toluidine blue reagent for 10 min. The analysis of the sections was carried out using a Microphot-FX microscope (Nikon Instruments Inc., Tokyo, Japan) equipped with a Digital Sight DS-5 M camera.

3.8. Determination of collagen content

To detect collagen deposition in rat cartilage tissue, the Total Collagen Assay kit (Perchlorate-Free) (ab222942, Abcam) was utilized following the provided instructions. In summary, the cartilage tissues were prepared as homogenates and then centrifuged at 1407 g for 10 min to remove the precipitate. The supernatant was collected and treated with 10N sodium hydroxide for alkaline hydrolysis for 30 min. Subsequently, the oxidation reagent mix was added and incubated at 37 °C for 25 min. After the addition of DMAB, the mixture was incubated at 65 °C for 45 min. The optical density (OD) value at 560 nm (OD560) was measured using a microplate reader to quantify the collagen content in the samples.

3.9. Statistical analysis

SPSS version 22.0 (IBM Corp. Armonk, NY, USA) was used for statistical analysis. Measurement data are expressed as the mean ± SD. Differences between groups were analyzed by the unpaired *t*-test, or by

one- or two-way ANOVA followed by Tukey's post-hoc test when over two groups were concerned. *P* < 0.05 is indicative for statistically significant difference.

4. Results

4.1. IRF1 is a regulon of SMARCC1 that potentially participates in the onset and development of OA

The scRNA-seq dataset GSE152805 which contains single-cell transcriptome data of three pairs of cartilage tissues and synovium was downloaded from GEO database and analyzed. The "Seurat" R package was used for quality control. The data were standardized using the logNormalize method and integrated by canonical correspondence analysis (CCA). A total of 36,832 cells were obtained, including 10,640 synovial cells and 26,192 chondrocytes. Thereafter, the cells were annotated and classified into eight subtypes (Fig. 1A–B). The "FindVariableFeatures" function was performed to identify 2000 differentially expressed genes (DEGs) in OA chondrocytes, and a volcano plot for these DEGs was plotted by the findmarker function and Wilcoxon test. Afterward, we performed gene set variation analysis (GSVA) to analyze the gene variations in chondrocytes according to the Hallmarker gene set, with the IL-10 and TNF- α -via-NF κ B signaling pathway identified (Fig. 1C–D). Furthermore, based on the DEGs in Fig. 1D, we observed that IRF1 and SMARCC1 were highly expressed in chondrocytes in an OA condition (Fig. 1E–F). Therefore, we hypothesize that IRF1 regulates the expression of SMARCC1 as a Regulon, thereby activating the NF κ B signaling pathway in macrophages and promoting the binding of p65/p50 to the nucleus, further promoting the production of downstream inflammatory factors such as TNF α and IL-1 β , and triggering the occurrence and development of OA. To confirm the regulatory effect of IRF1 on SMARCC1, we downloaded IRF1's ChIP-seq data from the

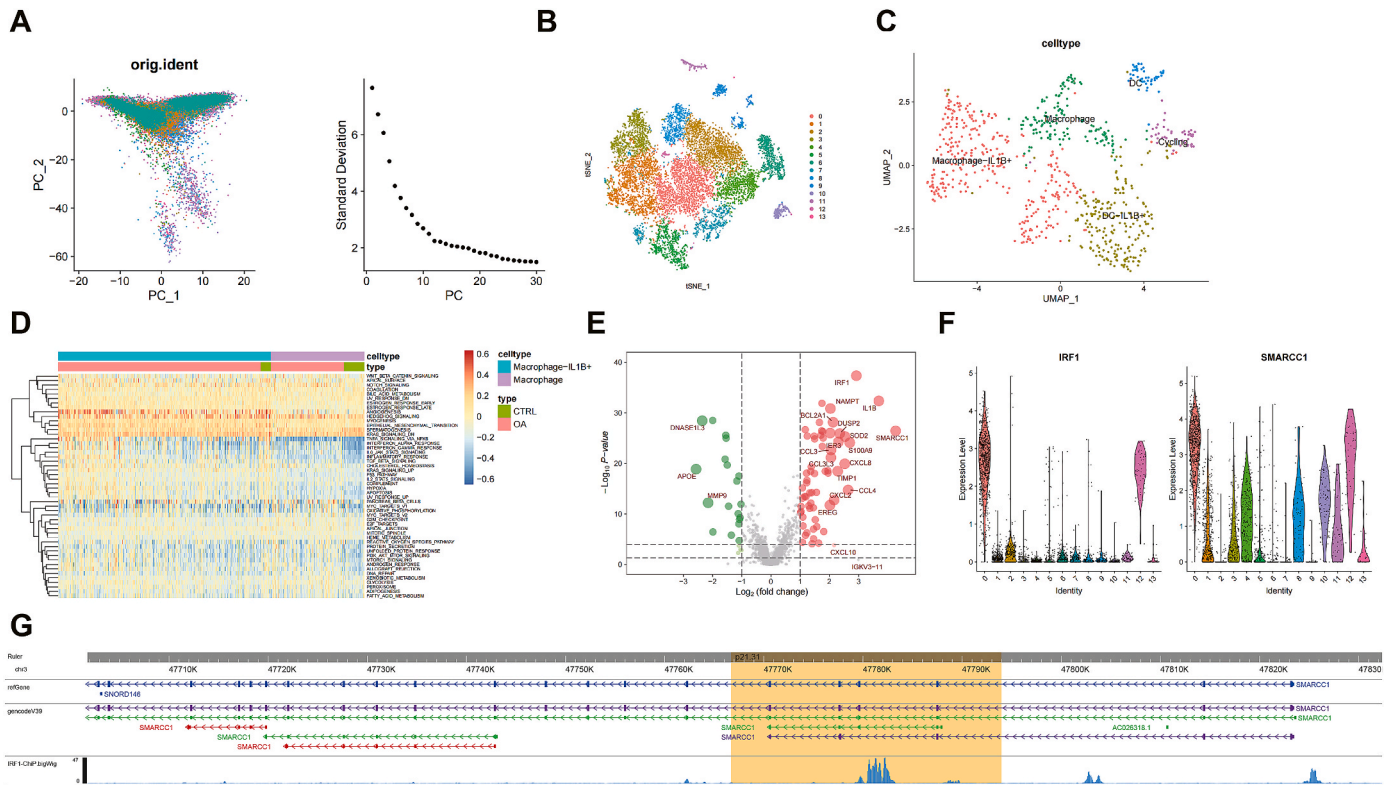


Figure 1. IRF1 is a regulon of SMARCC1 that potentially participates in the onset and development of OA. A-B, cell types differing in control and CCA groups in GSE152805 dataset; C, DEGs between OA- and non-OA-chondrocytes and the volcano plots generated by the findmarker function wilcoxon test; and to find differential genes and plot volcanoes; D, gene variation analysis to screen relevant signaling pathways in two types of macrophages based on the Hallmarker gene set; E-F, differential expression levels of IRF1 and SMARCC1 in OA; G, the regulatory role of IRF1 on SMARCC1 confirmed by ChIP-seq analysis.

ENCODE database and performed dimensionality reduction of the data by model-based analysis of ChIP-Seq (MACS2) and Bowtie-2 for data visualization using the Integrative Genomics Viewer. Of note, a clear PEAK of IRF1 near the SMARCC1 promoter on the Hg19 genome (Fig. 1G). The results fully demonstrate that IRF1 can regulate the expression of SMARCC1 as a Regulon.

4.2. Knockdown of SMARCC1 or IRF1 impairs the pro-inflammatory effect of IL-1 β on chondrocytes

To validate the expression profiles and functions of IRF1 and SMARCC1 in OA, we treated the chondrocytes with IL-1 β to mimic the OA condition in vivo, where significantly elevated expression of IRF1 and SMARCC1 were detected (Fig. 2A–B). Thereafter, lentivirus vectors-carried sh-IRF1 or sh-SMARCC1 was introduced in the IL-1 β -stimulated chondrocytes, which successfully suppressed the mRNA and protein levels of IRF1 or SMARCC1 in the cells. Meanwhile, the sh-IRF1 also suppressed the expression of SMARCC1 (Fig. 2C–D). The CCK-8 and EdU assays revealed that the viability and proliferation of chondrocytes were suppressed by IL-1 β stimulation but then restored by artificial IRF1 or SMARCC1 knockdown (Fig. 2E–F). The TUNEL assay revealed that the

number of apoptotic bodies in the chondrocytes was increased by IL-1 β stimulation but reduced by IRF1 or SMARCC1 silencing (Fig. 2G). The RT-qPCR and WB concerning the expression of extracellular matrix (ECM)-related factors in the chondrocytes showed that the levels of matrix genesis-related (Aggrecan and Collagen II) was decreased whereas the level of matrix degradation-related MMP13 was increased upon IL-1 β treatment. Of note, the mRNA and protein levels of these factors were partly restored to normal levels after IRF1 or SMARCC1 knockdown (Fig. 2H–I). Moreover, the ELISA results showed that the production of IL-6 and TNF- α in the culture medium of chondrocytes was increased by IL-1 β stimulation but decreased by IRF1 or SMARCC1 shRNA (Fig. 2J).

4.3. IRF1 regulates M1-type polarization of macrophages via SMARCC1

Macrophages are key immune cells closely linked to the progression of inflammatory damage in OA. Here, to clarify the effect of the IRF1-SMARCC1 axis on macrophage polarization, we first induced M0 macrophages (PMA-treated THP-1 monocytes) and then had them co-cultured with the IL-1 β -treated chondrocytes (Fig. 3A). The RT-qPCR and WB analysis showed that co-culturing with the IL-1 β -treated

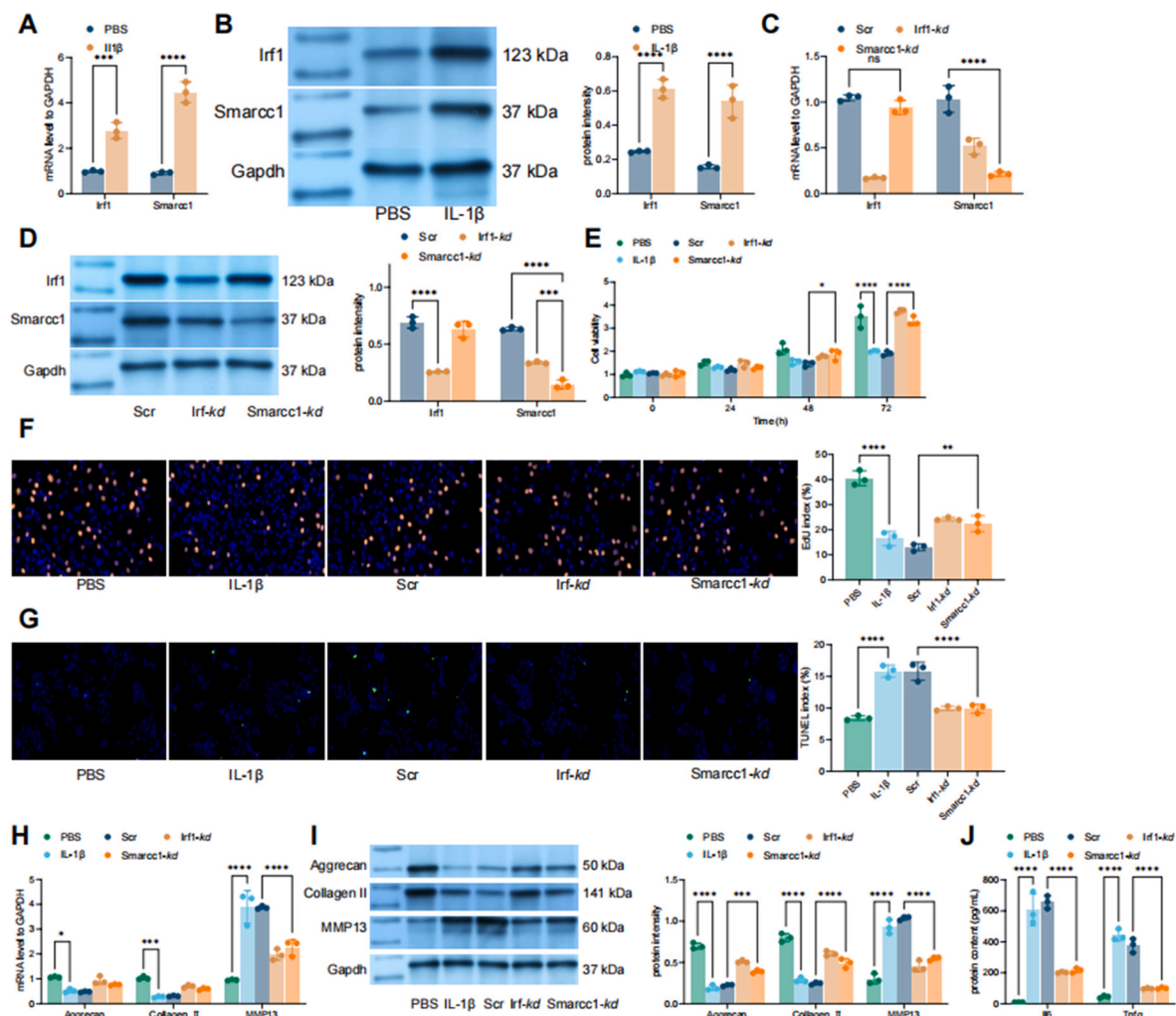


Figure 2. Knockdown of SMARCC1 or IRF1 impairs the pro-inflammatory effect of IL-1 β on chondrocytes. A–B, mRNA and protein expression of SMARCC1 and IRF1 in IL-1 β -stimulated chondrocytes detected by RT-qPCR and WB analysis; C–D, mRNA and protein expression of SMARCC1 and IRF1 in IL-1 β -stimulated chondrocytes after SMARCC1 or IRF1 treatment detected by RT-qPCR and WB analysis; E–F, viability and proliferation of the chondrocytes evaluated by CCK-8 and EdU labeling assays; G, number of apoptotic bodies in the chondrocytes determined by TUNEL assay; H–I, mRNA and protein levels of ECM production- or degradation-related factors in the chondrocytes determined by RT-qPCR and WB analysis; J, production of inflammatory factors IL-6 and TNF- α in the culture medium of chondrocytes detected by ELISA kits. Three biological replicates were performed. Differences were analyzed by the one- or two-way ANOVA followed by Tukey’s multiple comparison test. ** $P < 0.01$, *** $P < 0.001$.

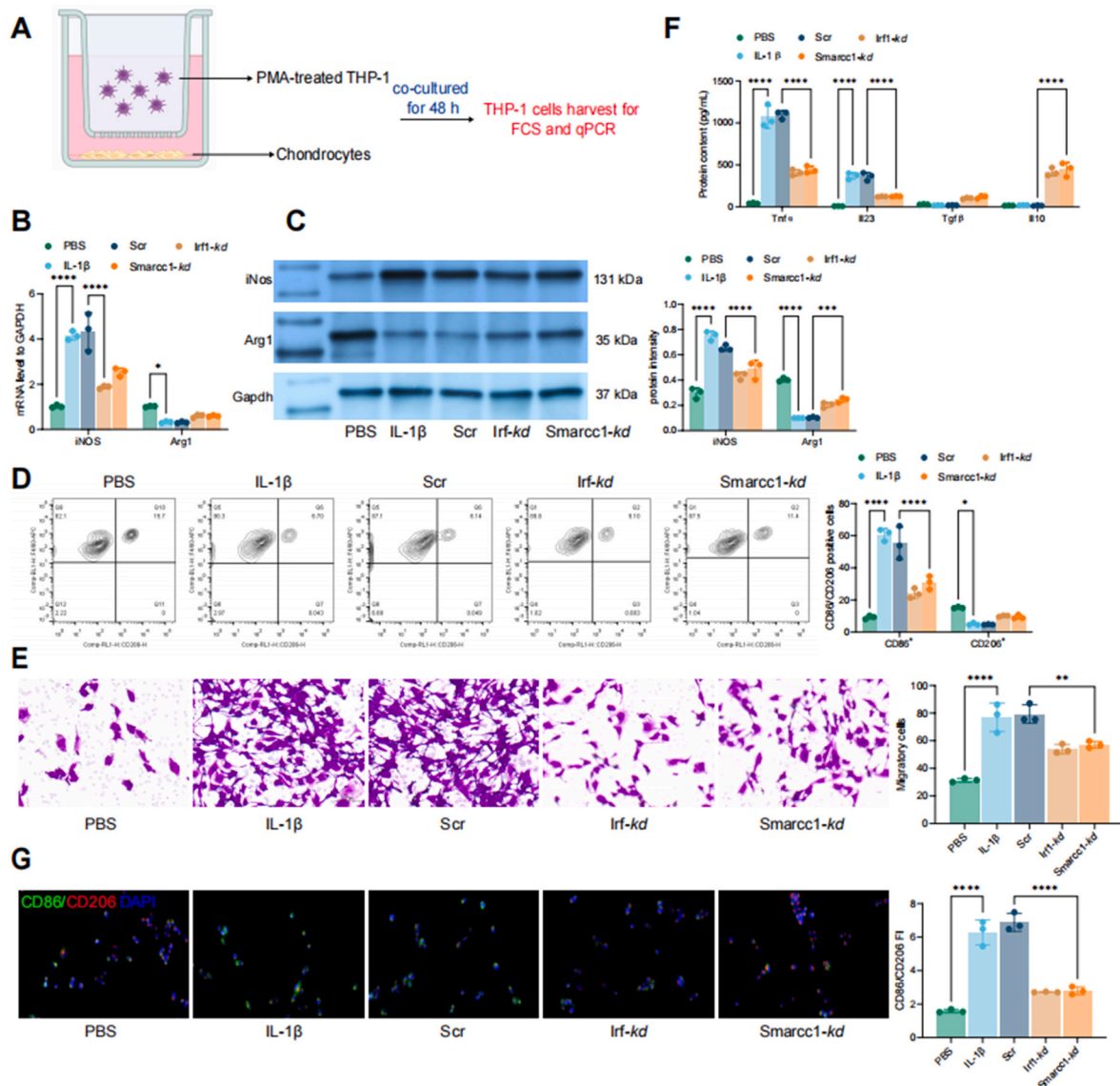


Figure 3. IRF1 regulates M1-type polarization of macrophages via SMARCC1. A, a diagram for the co-culture system of M0 macrophages (PMA-treated THP-1 monocytes) and IL-1 β -treated chondrocytes; B–C, mRNA and protein levels of M1 marker iNOS and M2 marker Arg1 in the macrophages determined by RT-qPCR or WB analysis; D, the proportions of M1 macrophages (CD86⁺) and M2 macrophages (CD206⁺) in the co-culture system analyzed by flow cytometry; E, chemotactic migration of macrophages in the co-culture system determined by Transwell assay; F, expression of M1-type cytokines (TNF- α and IL-23) and M2-type cytokines (IL-10 and TGF- β) in the culture medium analyzed by ELISA kits; G, proportion of M1/M2 macrophages (CD86/CD206) analyzed by dual-label immunofluorescence staining. Three biological replicates were performed. Differences were analyzed by the one- or two-way ANOVA followed by Tukey's multiple comparison test. ** $P < 0.01$, *** $P < 0.001$.

chondrocytes led to an increase in the M1 marker iNOS whereas a decline in the M2 marker Arg1 in the macrophages. However, the IRF1 or SMARCC1 silencing reversed the predominance of M1 macrophages (Fig. 3B–C). The flow cytometry similarly showed that the ratio of M1/M2 macrophages was increased when they were co-cultured with IL-1 β -treated chondrocytes but then decreased when IRF1 or SMARCC1 shRNA was administered (Fig. 3D). Moreover, the Transwell assay also showed that the IL-1 β treatment in chondrocytes promoted whereas the IRF1 or SMARCC1 silencing suppressed the chemotactic migration of macrophages (Fig. 3E). ELISA results also showed that the production of M1-type cytokines (TNF- α and IL-23) was increased but the M2-type cytokines (IL-10 and TGF- β) were declined when co-cultured with the IL-1 β -treated chondrocytes. Still, knockdown of IRF1 or SMARCC1 in the chondrocytes led to inverse trends (Fig. 3F). The dual-label immunofluorescence staining of CD86 and CD206 showed similar trends that the M2 polarization of macrophages was suppressed by IL-1 β but restored by

IRF1 or SMARCC1 silencing (Fig. 3G).

4.4. Knockdown of SMARCC1 or IRF1 alleviates OA-like symptoms in rats

To further verify the effect of SMARCC1 or IRF1 on OA, we established a rat model of OA and treated them with lentivirus vector-carried shRNA targeting IRF1 or SMARCC1 once every 5 d until the end point of the experiment (Fig. 4A). The IRF1 or SMARCC1 silencing alleviated the OA-like symptoms in rats according to the Safranin O staining and Mankin scoring (Fig. 4B), and it decreased the concentrations of inflammatory cytokines in the synovial fluid (Fig. 4C). The cartilage tissues of knee joint were collected for toluidine blue staining. Of note, the cartilage degeneration in model rats was significantly mitigated by the IRF1 or SMARCC1 knockdown (Fig. 4D). Meanwhile, the HE and Safarin and fast green staining suggested that the shRNA of IRF1 or SMARCC1

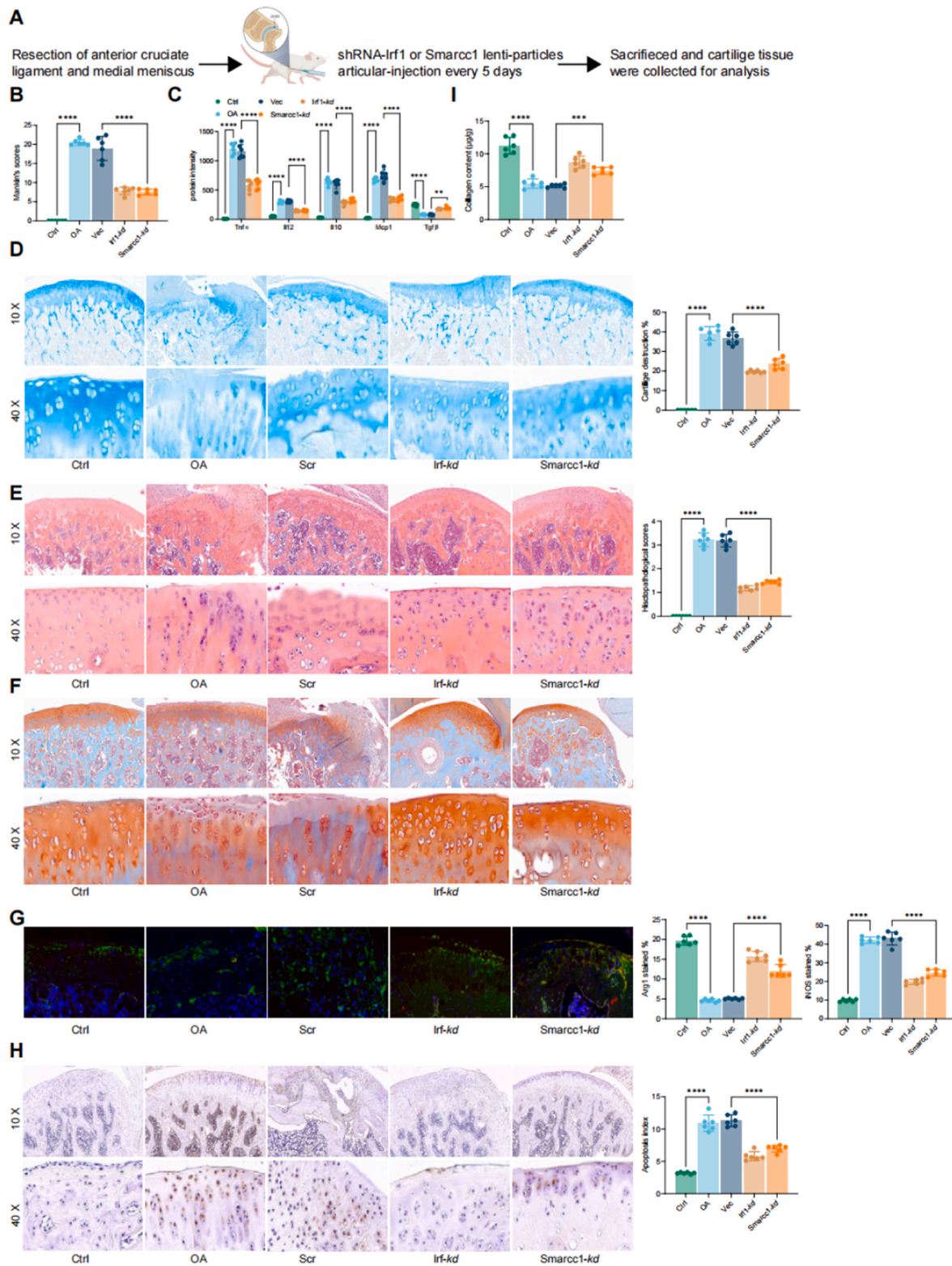


Figure 4. Knockdown of SMARCC1 or IRF1 alleviates OA-like symptoms in rats. A, a diagram for rat model establishment and treatment; B, OA-like symptoms in rats determined by Safranin O staining and Mankin scoring; C, concentrations of TNF- α , IL-12, IL-10, MCP-1 and TGF- β in the synovial fluid examined by ELISA kits; D, cartilage degeneration in rats examined by toluidine blue staining; E ~ F, pathological changes and inflammatory cell infiltration in the cartilage tissue examined by HE and safranin and fast green staining; G, expression of the M1-type protein iNOS and M2-type protein Arg1 in the cartilage tissue determined by immunofluorescence; H, apoptotic cells in the cartilage tissue examined by TUNEL assay; I, collagen content in the cartilage examined using a collagen deposition kit. In each group, n = 6. In the graphs, each spot refers to a rat. Differences were analyzed by the one- or two-way ANOVA followed by Tukey's multiple comparison test. ** $P < 0.01$, *** $P < 0.001$. (For interpretation of the references to color in this figure legend, the reader is referred to the Web version of this article.)

reduced the tissue injury and inflammatory cell infiltration in the cartilage tissue (Fig. 4E ~ F). Similar to the results *in vitro*, we identified increased number of iNOS-positive cells whereas reduced Arg1-positive cells in the rat cartilage according to immunofluorescent results (Fig. 4G). The TUNEL assay also suggested that the number of apoptotic cells in the cartilage tissue was reduced by IRF1 or SMARCC1 silencing (Fig. 4H). Moreover, the collagen content in the cartilage was increased as well (Fig. 4I).

4.5. IRF1 recruits H3K27ac and H3K4me3 modifications to activate SMARCC1 expression

To further unravel the mechanism for the high expression of SMARCC1 in OA, we downloaded the GEO dataset GSE112655 that contains the ChIP-seq data of H3K27ac, H3K36me3, H3K4me1, H3K4me3, and H3K9me3 from 11 OA patients. We found that the modification levels of H3K27ac, H3K4me3, and H3K9me3 were significantly increased in OA by MACS2 and call 4 peaks analysis (Fig. 5A). Thereafter, the Bigwig format data were visualized and analyzed by IGV software and localized to chr3:47,585,269. Of note, we observed that SMARCC1 had significant enrichment of H3K27ac and H3K4me3 modifications around 10 kb upstream (Fig. 5B). Afterward, ChIP-qPCR was performed to verify the regulatory role of H3K27ac and H3K4me3 modifications on SMARCC1. Both in the extracted rat chondrocytes and cartilage tissues, abundant SMARCC1 fragments were enriched in the complexes pulled down by the H3K27ac and H3K4me3 antibodies compared to IgG (Fig. 5C). Similar results were observed in the IL-1 β -treated chondrocytes (Fig. 5D). Further, we treated the chondrocytes with the histone acetyltransferase inhibitor MG149 and the histone methyltransferase inhibitor BRD9359, after which the mRNA and protein levels of SMARCC1 were significantly reduced. The expression of IRF1 was, however, not significantly affected (Fig. 5E–F).

4.6. GCN5-SETD2 is involved in epigenetic regulation of SMARCC1 expression

To identify the enzymes that modify epigenetic marks involved in

regulating SMARCC1 expression, a library of histone acetyltransferase and methyltransferase inhibitors were purchased from Selleck Chemicals (Houston, TX, USA) for screening. It was found that the treatments of YF-2, SR-18292, UNC0646, A366, and EZM0414 small molecules, which target CBP, PCAF, GCN5, G9a, SETD2 proteins, led to the most significant decrease in SMARCC1 mRNA levels in chondrocytes (Fig. 6A). Afterward, the expression of CBP, PCAF, GCN5, G9a, and SETD2 were examined in rat cartilage tissues and in the isolated chondrocytes. Of note, the GCN5 and SETD2 levels were significantly increased in cartilage tissues of OA rats or IL-1 β -treated chondrocytes (Fig. 6B–C). Therefore, we conjectured that GCN5 and SETD2 affect the expression of SMARCC1 by regulating the H3K27ac-H3K4me3 modifications, thus exacerbating the OA symptoms. The ChIP-qPCR was performed thereafter, which showed that the GCN5 and SETD2 GCN5 and SETD2 antibodies enriched for abundant SMARCC1 promoter fragments (Fig. 6D). Additionally, a pGL3-E-Luc luciferase reporter vector containing the 10 kb sequence upstream of the promoter of SMARCC1 was constructed and co-transfected with GCN5 and SETD2 overexpression vectors into 293T cells, which resulted in a significant increase in luciferase activity in the cells (Fig. 6E). Moreover, we induced GCN5 and SETD2 overexpression in chondrocytes, which led to a conspicuous upregulation of SMARCC1 (Fig. 6F–G). To further confirm the recruitment of GCN5 or SETD2 by IRF1, we conducted a double-label immunofluorescence experiment. In chondrocytes, we observed that IRF1 has binding interactions with both GCN5 and SETD2 (Fig. 6H). Subsequently, we performed ChIP experiments in cells with IRF1 knockdown and found a significant reduction in the binding of GCN5 or SETD2 to the SMARCC1 promoter (Fig. 6I). These results suggest that GCN5 and SETD2 are involved in the regulation of SMARCC1 and the progression of OA.

4.7. Overexpression of GCN5 or SETD2 impairs the attenuating effect of sh-SMARCC1 on OA symptoms

To confirm the functions of GCN5 and SETD2 in OA, we further induced GCN5 or SETD2 overexpression in OA rats with stable SMARCC1 knockdown (Fig. 7A). The GCN5 or SETD2 overexpression

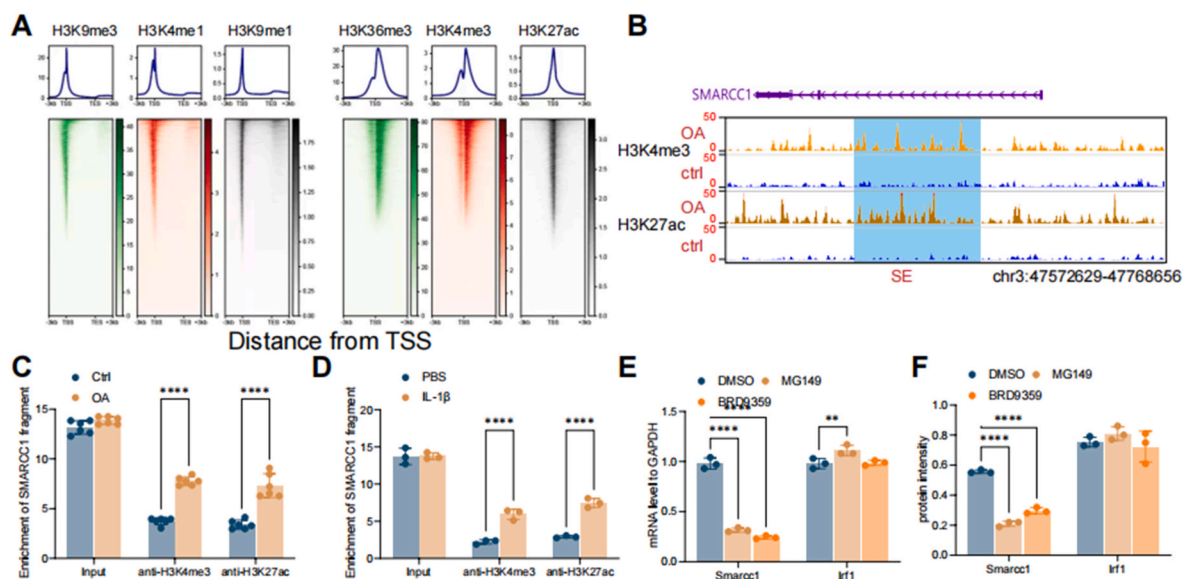


Figure 5. IRF1 recruits H3K27ac and H3K4me3 modifications to regulate SMARCC1 expression. A–B, enrichment of H3K27ac, H3K36me3, H3K4me1, and H3K4me3 modifications in the genome of 11 OA patients according to MACS2 and call 4 peaks analysis of the GSE112655 ChIP-seq dataset; C–D, binding relationships between H3K27ac and H3K4me3 and the promoter of SMARCC1 and its upstream 10 kb in rat cartilage or in the extracted chondrocyte determined by ChIP-qPCR; E–F, mRNA and protein levels of SMARCC1 and IRF1 in chondrocytes after MG149 or BRD9359 treatment detected by RT-qPCR and WB analysis. For cellular experiments, three biological replicates were performed. For animal studies, n = 6 in each group. Differences were analyzed by the one- or two-way ANOVA followed by Tukey's multiple comparison test. ** $P < 0.01$, *** $P < 0.001$.

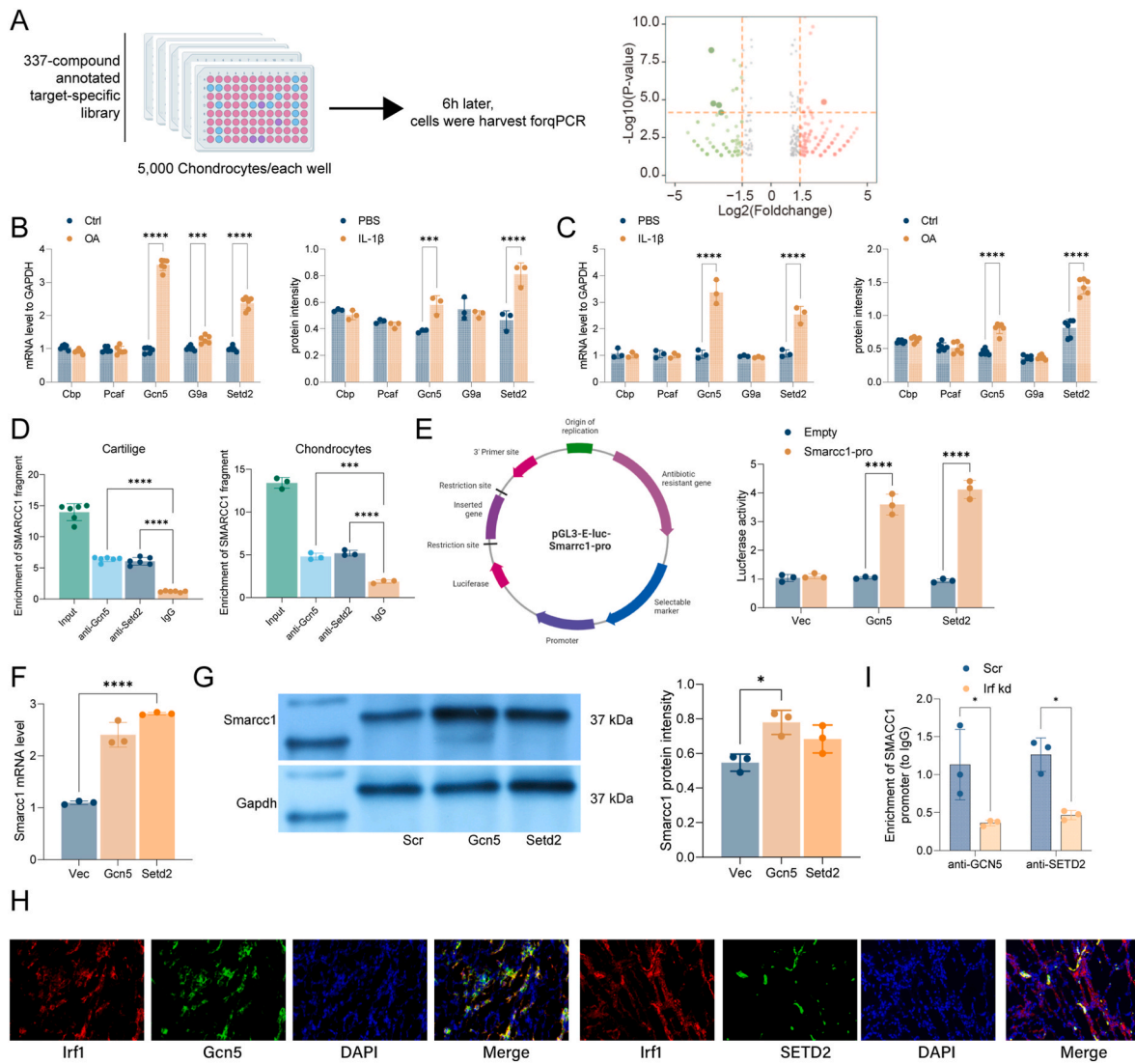


Figure 6. GCN5-SETD2 is involved in epigenetic regulation of SMARCC1 expression. A, RT-qPCR for SMARCC1 mRNA expression in chondrocytes after treatment of a library of commercial histone modification compounds; B–C, mRNA and protein levels of CBP, PCAF, GCN5, G9a, SETD2 in rat cartilage tissues and in the isolated chondrocytes examined by RT-qPCR and WB analysis; D, binding relationship of GCN5 and SETD2 with the SMARCC1 promoter and its upstream 10 kb in rat cartilage tissues and chondrocytes detected by ChIP-qPCR assay; E, construction of pGL3-E-Luc luciferase reporter vector containing the 10 kb sequence upstream of the promoter of SMARCC1 to examine the effect of GCN5 and SETD2 overexpression on the luciferase activity in 293T cells; F–G, mRNA and protein expression of SMARCC1 in chondrocytes after GCN5 and SETD2 overexpression determined by RT-qPCR and WB analysis. H, Fluorescence co-localization experiments confirmed the binding relationship between IRF1 and Gcn5 as well as SETD2. I, ChIP experiments validated the binding relationship of Gcn5 and Setd2 with Smarcc1 in chondrocytes following the knockdown of Irf1. For cellular experiments, three biological replicates were performed. For animal studies, $n = 6$ in each group. Differences were analyzed by the one- or two-way ANOVA followed by Tukey's multiple comparison test. $**P < 0.01$, $***P < 0.001$.

conspicuously exacerbated the OA symptoms (Fig. 7B), and it promoted the tissue injury, inflammatory infiltration, and cartilage degradation in the model rats (Fig. 7C–D), accompanied by an increase in iNOS-positive cells whereas a reduction in Arg1-positive cells (Fig. 7E). Meanwhile, the GCN5 or SETD2 overexpression increased the proportion of apoptotic cells in the cartilage tissue (Fig. 7F), along with a conspicuous elevation of the levels of inflammatory factors TNF- α , IL-12, IL-10, MCP-1, and TGF- β in the synovial fluid (Fig. 7G). As expected, increased SMARCC1 mRNA and protein levels were detected in rat cartilage tissues after the GCN5 or SETD2 overexpression (Fig. 7H ~ I).

4.8. SMARCC1 expression is significantly increased in cartilage tissue of clinical OA patients

To analyze the clinical translation value of the IRF1-GCN5-SETD2-SMARCC1 axis, we collected cartilage tissues from 13 patients with

OA and another 7 patients without. Importantly, the RT-qPCR assays identified significantly elevated IRF1, GCN5, SETD2 and SMARCC1 levels in the OA-diseased cartilage tissues compared to the controls (Fig. 8A). The patients' Mankin's scores were positively correlated with the levels of IRF1, GCN5, SETD2 and SMARCC1 (Fig. 8B). Moreover, the Spearman's correlation analysis showed that the expression levels of IRF1, GCN5, SETD2 and SMARCC1 were significantly positively correlated (correlation coefficient $R > 0.35$) (Fig. 8C). Moreover, we further induced GCN5 or SETD2 overexpression in chondrocytes with SMARCC1 knockdown, after which a significant inhibition of cell viability and an increase in the proportion of apoptotic cells were observed (Figs. S1A–D). Meanwhile, the GCN5 or SETD2 overexpression significantly increased the MMP13 expression but decreased Aggrecan expression in the chondrocytes (Fig. S1E), accompanied by an increased polarization ratio of M1 macrophages and a decreased ratio of M2 macrophages in the co-culture system (Figs. S1F–H). In summary, we

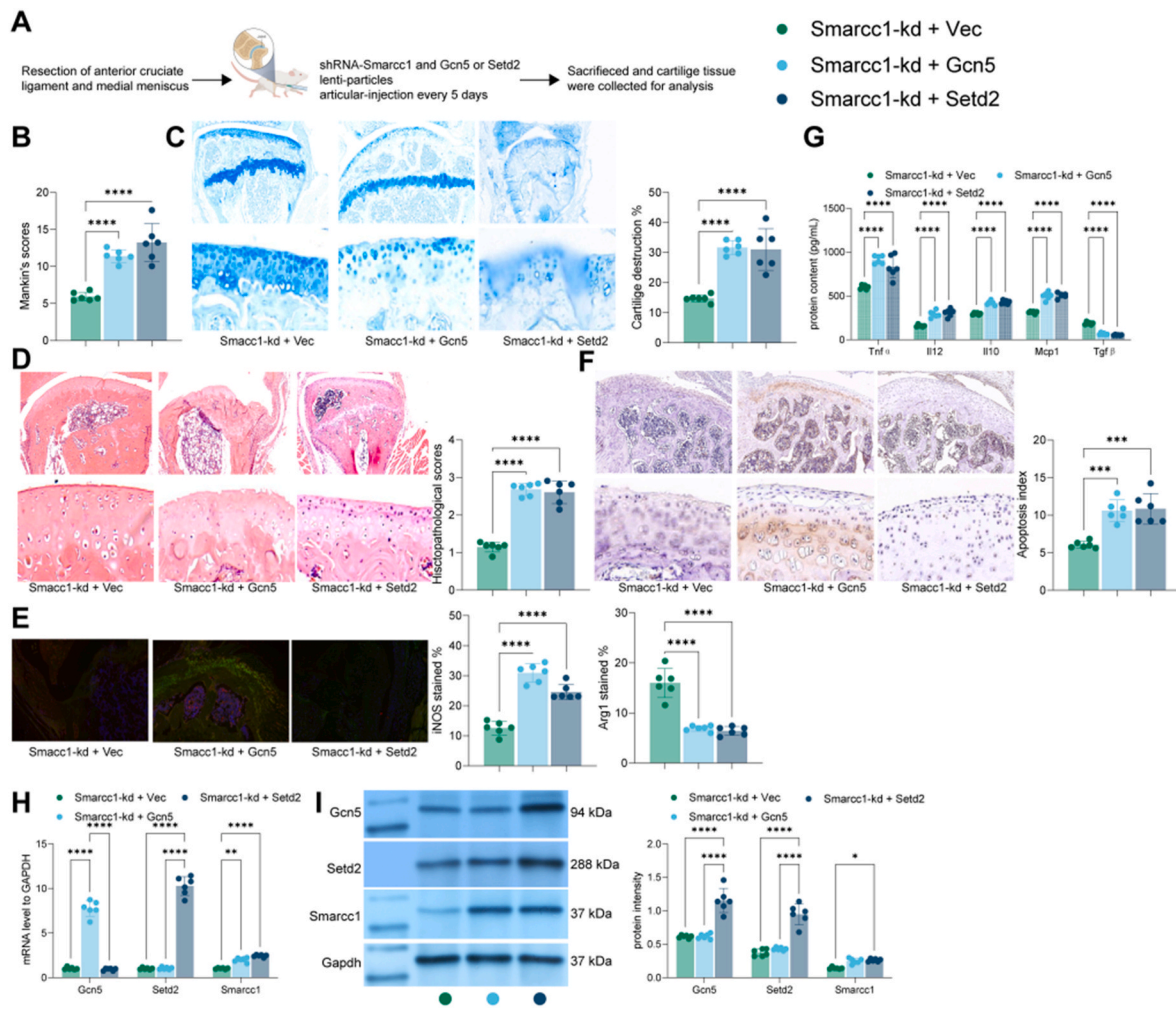


Figure 7. Overexpression of GCN5 or SETD2 impairs the attenuating effect of sh-SMARCC1 on OA symptoms. A, a diagram for animal treatment; B, OA-like symptoms in rats determined by Safranin O staining and Mankin scoring; C, cartilage degeneration in rats examined by toluidine blue staining; D, pathological changes and inflammatory cell infiltration in the cartilage tissue examined by HE staining; E, expression of the M1-type protein iNOS and M2-type protein Arg1 in the cartilage tissue determined by immunofluorescence; F, apoptotic cells in the cartilage tissue examined by TUNEL assay; G, concentrations of TNF- α , IL-12, IL-10, MCP-1 and TGF- β in the synovial fluid examined by ELISA kits; H ~ I, mRNA and protein levels of GCN5, SETD2, and SMARCC1 in rat cartilage tissues analyzed by RT-qPCR and WB analysis. In each group, $n = 6$. In the graphs, each spot refers to a rat. Differences were analyzed by the one- or two-way ANOVA followed by Tukey's multiple comparison test. $**P < 0.01$, $***P < 0.001$. (For interpretation of the references to color in this figure legend, the reader is referred to the Web version of this article.)

opine that IRF1 can influence the transcriptional activation of SMARCC1 by recruiting histone modifying enzymes SETD2 and GCN5, which ultimately contributes to the development and progression of osteoarthritis symptoms (Fig. 9).

5. Discussion

While conventional treatment options for osteoarthritis (OA), including physical therapy, oral medications, lifestyle modifications, injections, physical modalities, and surgical interventions, have demonstrated efficacy in relieving symptoms, it is important to note that there is currently no definitive cure for OA. These interventions primarily aim to manage pain, improve joint function, and slow down the progression of the disease. However, they do not offer a permanent solution to reverse or eliminate OA completely. Ongoing research efforts are focused on developing novel therapeutic approaches that could potentially offer a curative treatment for OA in the future [22]. The growing need for effective therapeutic strategies in osteoarthritis (OA) has led researchers and clinicians to explore additional molecular factors involved in OA pathogenesis and develop potential drug candidates. In

this study, the authors employed integrated bioinformatics analyses and generated in vitro and in vivo OA models. Their findings revealed that IRF1 plays a crucial role in activating SMARCC1 transcription by facilitating GCN5 and SETD2-dependent modifications, namely 2H3K27ac and H3K4me3, near the SMARCC1 promoter and 10 kb upstream region. Consequently, these modifications resulted in increased M1 polarization of macrophages and exacerbated symptoms of OA.

Chondrocytes are the sole cell type in articular cartilage, and loss or dysfunction of chondrocytes is a major pathological feature of OA [23]. They play special and independent roles in the maintenance and turnover of ECM-related molecules including Aggrecan, collagen II, and non-collagenous proteins [24]. Research in OA has paid attention to changes in cartilage matrix, inflammatory mediators, and loss of cartilage chondrocytes [25]. Based on the insights gained from the bioinformatics analysis, a significant increase in the expression of IRF1 and SMARCC1 was observed in the articular cartilage of rats with osteoarthritis (OA) and IL-1 β -stimulated chondrocytes. Of particular importance is the recognition of IRF1 as a crucial pro-inflammatory transcription factor that is active in TNF- α -activated chondrocytes. These findings provide compelling evidence for the potential

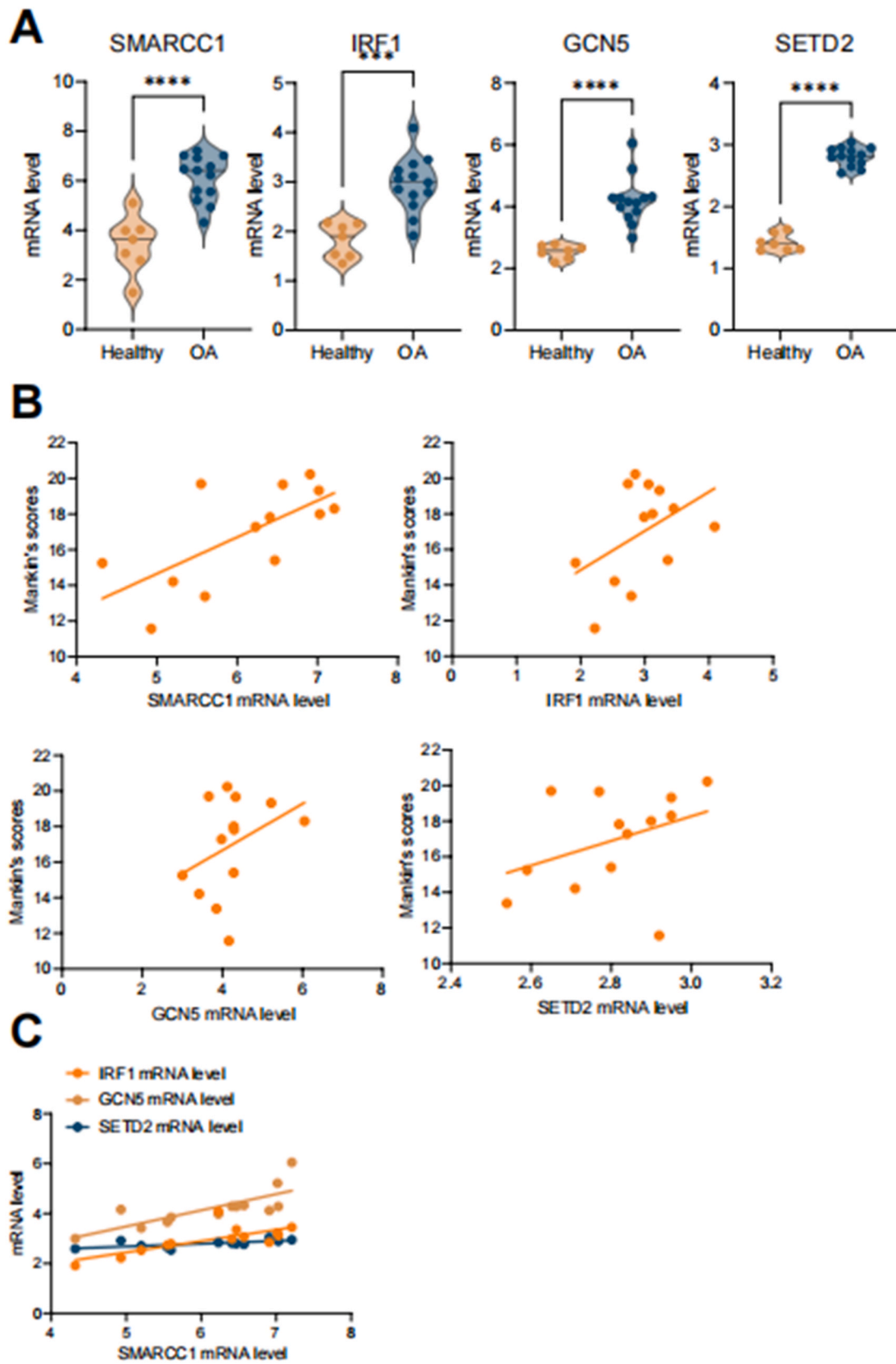


Figure 8. SMARCC1 expression is significantly increased in cartilage tissue of clinical OA patients. A, expression of IRF1, GCN5, SETD2 and SMARCC1 in cartilage tissues from 13 patients with OA and another 7 patients without detected by RT-qPCR; B, correlations of the Mankin's score of OA patients with the detected IRF1, GCN5, SETD2 and SMARCC1 expression levels; C, correlation between IRF1, GCN5, SETD2 and SMARCC1 expression levels analyzed by Spearman correlation analysis. In panels A–C each point represents one subject. Differences were analyzed by the one- or two-way ANOVA followed by Tukey's multiple comparison test. ** $P < 0.01$, *** $P < 0.001$.

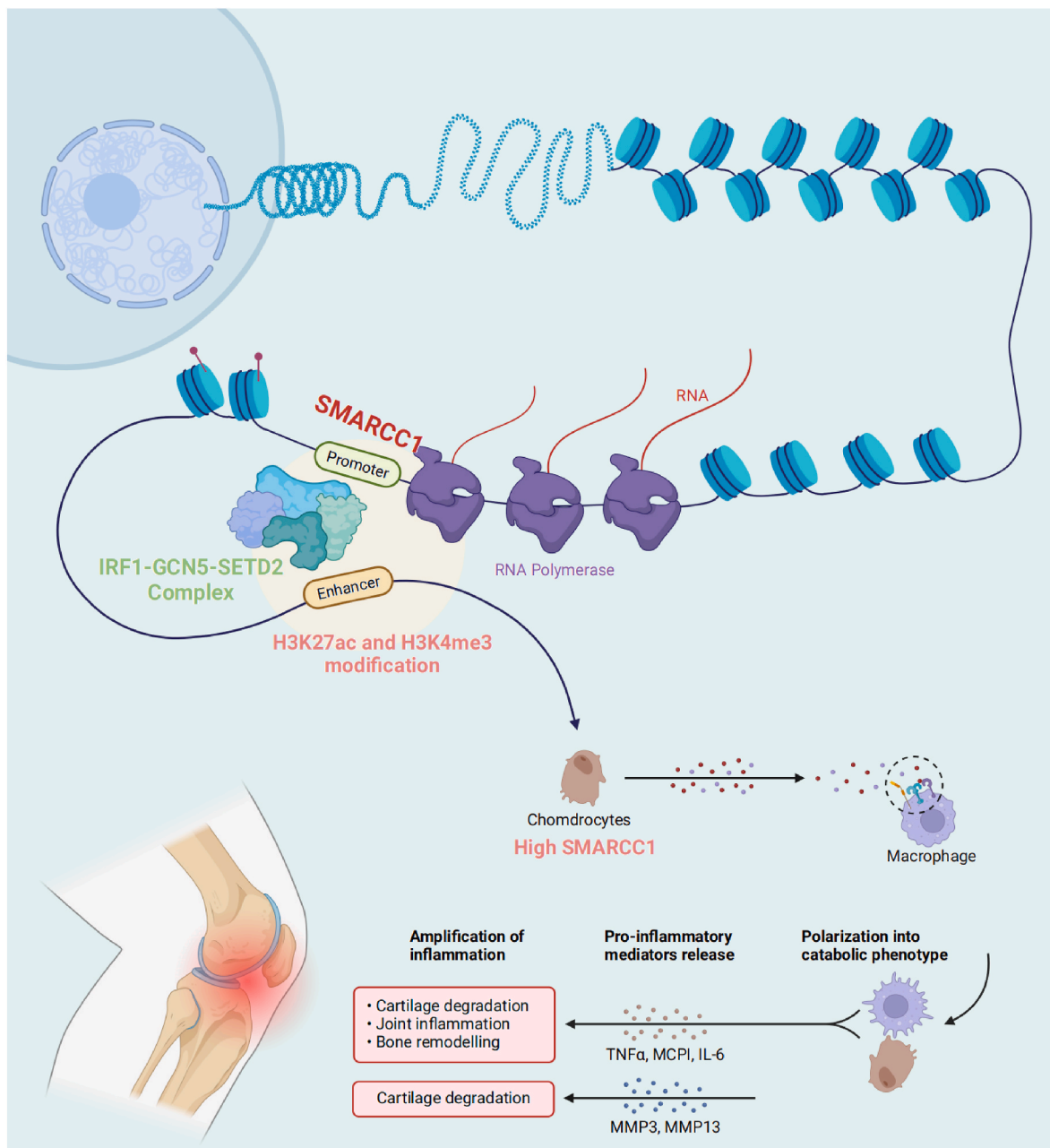


Figure 9. The transcriptional activity of SMARCC1 can be influenced by IRF1 through the recruitment of GCN5 and SETD2, consequently regulating the H3K27ac and H3K4me3 modifications in close proximity to the SMARCC1 promoter.

involvement of IRF1 and SMARCC1 in the inflammatory mechanisms underlying the development and progression of osteoarthritis [26]. Similarly, in the previous work by Liu et al. [27], inhibition showed specific correlation with the IL-1 β -induced ECM degradation in human chondrocytes. Here, our functional experiments clearly identified that either knockdown of IRF1 or SMARCC1 suppressed the OA symptoms in the cartilage, reduced the apoptosis of chondrocytes, and decreased the ECM degradation. The chronic inflammation is the primary cause for OA. It induces cartilage degradation, which in turn triggers increased production of inflammatory cytokines and further cartilage destruction [22]. The observed decrease in the secretion of inflammatory cytokines following the silencing of IRF1 or SMARCC1 in both experimental models provides further confirmation of the causal relationship between these two molecules and the progression of osteoarthritis (OA). It is noteworthy that the increased prevalence of M1 macrophages is widely acknowledged as a significant factor contributing to the accumulation of

inflammation during the development of OA [10,28]. IRF1 has reportedly been linked to the M1 polarization of macrophages in several inflammatory conditions [29–31]. Our investigation revealed that IRF1 plays a role in promoting M2 skewing of macrophages. However, limited evidence exists regarding the specific function of SMARCC1 in chondrocyte function or the development of osteoarthritis (OA). Notably, a study conducted by LEE et al. reported that the overexpression of SRG3, the mouse homolog of human SMARCC1, likely induced Th2 response and M2 skewing of macrophages, resulting in variable effects on disease conditions, potentially improving or worsening them [20,32,33]. Interestingly, they also found that the specific SRG3 overexpression resulted in increased Th1 responses that is linked to M1 polarization [33]. However, we clearly identified that the SMARCC1 knockdown triggered a M1-to-M2 shift of the macrophages. The discrepancy indicates that the function of SMARCC1 in the macrophage phenotype may be distinct in different disease conditions, and the detailed

mechanisms remain to be elucidated yet.

In eukaryotes, the regulation of gene expression is a complex process that involves the interplay of genetic and epigenetic factors. Epigenetic mechanisms, including histone modifications, DNA methylation, and chromatin remodeling, play essential roles in governing gene expression patterns and influencing various biological processes such as development, regeneration, and oncogenesis. These epigenetic regulations act as crucial mechanisms for fine-tuning gene expression and ensuring the proper functioning of cells and organisms [34]. The aberrant epigenetic regulation is also applied in the pathogenesis of OA [35]. Of note, we identified abundant H3K27ac and H3K4me3 modifications at 10 kb upstream of the SMARCC1 promoter. These two histone markers are indicative of active promoters that are linked to active transcription [36]. The observed reduction in SMARCC1 mRNA and protein levels following treatment with MG149 or BRD9359 indicates that the abnormal upregulation of SMARCC1 in osteoarthritis (OA) is associated with elevated H3K27ac and H3K4me3 modifications. The enzymes responsible for these modifications were investigated by introducing a library of inhibitors targeting histone acetyltransferases and methyltransferases. Among them, GCN5 and SETD2 exhibited the most significant downregulation in the cartilage of OA rats and IL-1 β -induced chondrocytes. GCN5, also known as KAT2A, is a well-studied acetyltransferase that plays dual roles as a histone acetyltransferase and lysine acetyltransferase. It plays critical functions in the epigenetic landscape and chromatin modification [37,38]. As for SETD2, it is a histone methyltransferase SETD2 specifically responsible for H3K36me3 modification and plays a critical role in maintaining genomic integrity and stability [39]. A noteworthy finding in our study was the observed artificial upregulation of SMARCC1 in rat cartilage and chondrocytes, which resulted in a significant restoration of its expression and subsequent exacerbation of osteoarthritis (OA)-like symptoms. This observation highlights the importance of SMARCC1 in the pathogenesis of OA. Moreover, our investigation revealed positive correlations between the components of the IRF1-GCN5-SETD2-SMARCC1 axis, suggesting an interdependency among these factors. These correlations were also associated with the severity of symptoms and disease progression in the clinical patient cohort. These findings emphasize the significance of the interactions between IRF1, GCN5, SETD2, and SMARCC1 in the context of OA, and their potential as targets for therapeutic interventions.

6. Conclusion

In summary, the present work demonstrates that IRF1 functions as a regulator of SMARCC1 during the progression of OA. IRF1 activates SMARCC1 transcription by recruiting the histone enzymes GCN5 and SETD2 to the 10 kb upstream of the SMARCC1 promoter and triggering the H3K27ac and H3K4me3 modifications, which consequently leads to M1 polarization of macrophages, hyperinflammation, chondrocyte damage, ECM degradation, and OA development. The findings of the present work might provide novel insights into the clinical management of OA. However, the detailed mechanisms by which SMARCC1 induces M1 skewing of macrophages remain unclear, and we would like to focus on this issue in the near future.

7. Limitation

In conclusion, while our research has made important strides in understanding the role of IRF1 and SMARCC1 in OA development, there are several avenues for further exploration to strengthen the clinical applicability and mechanistic understanding of these findings. This could ultimately lead to more effective therapeutic strategies for OA. Although we observed significant epigenetic modifications near the SMARCC1 promoter, more mechanistic insights into how these modifications regulate SMARCC1 expression are needed. Besides, The study effectively demonstrated the effects of IRF1 and SMARCC1 knockdown in a rat model. Still, it's crucial to establish the clinical relevance of these

findings by investigating their role in human OA and potentially exploring their diagnostic or therapeutic potential.

Declarations

Ethics approval

The study protocol was approved by the Institutional Review Board of our hospital. The clinical trials were performed in compliance with the Declaration of Helsinki. All included patients were informed and signed the consent form. All animal procedures were approved by the Animal Ethics Committee of our hospital and performed in adherence to the NIH Guide for the Care and Use of Laboratory Animals.

8. Consent for publication

Not applicable.

Funding

Acknowledgements This work was financially supported by a grant from The Medical and Health Science and Technology Program of Zhejiang Province, China (No: 2023KY989 and 2024KY1379), the Project of Zhejiang provincial plan for TCM science and technology, China (No: 2023ZR111), the Medical and Health Science and Technology Program of Hangzhou, China (No: A20230195) and Natural Science Foundation of Zhejiang Province, China (No: LBY24H290005) to Dong Wang. Project of Zhejiang provincial plan for TCM science and technology China (No: 2022ZB238) and Natural Science Foundation of Zhejiang Province China (No: LBY24H290005) to Hao Pan. Moreover, this project was also supported by the National Natural Science Foundation of China (NSFC) grants (No: 82274280) and Supported by Excellent Youth Foundation of Natural Science Foundation of Zhejiang Province China (No: LR23H270001) to Hongting Jin.

Availability of data and materials

The data that support the findings of this study are available from the corresponding authors upon reasonable request.

CRediT authorship contribution statement

Dong Wang and Hongting Jin: manuscript review, experimental design. Yujun Zhang and Wei Cheng: data acquisition, manuscript preparation. Liangping Zhang: data analysis, manuscript preparation, manuscript editing. Du He and Lan Zhao: statistical analysis. Li Zhu, Wei Zhang and Chengyue Zhu: Animal experiments and statistical analysis. Zhimin Miao: manuscript editing. Hang Zhu and Hao Pan: manuscript review.

Declaration of competing interest

The authors declare that they do not have any competing financial interests or relationships that might have affected their work.

Appendix A. Supplementary data

Supplementary data to this article can be found online at <https://doi.org/10.1016/j.jot.2024.01.002>.

References

- [1] Yan J, Ding D, Feng G, Yang Y, Zhou Y, Ma L, et al. Metformin reduces chondrocyte pyroptosis in an osteoarthritis mouse model by inhibiting NLRP3 inflammasome activation. *Exp Ther Med* 2022;23(3):222.

- [2] Qi A, Lin C, Zhou A, Du J, Jia X, Sun L, et al. Negative emotions affect postoperative scores for evaluating functional knee recovery and quality of life after total knee replacement. *Braz J Med Biol Res* 2016;49(1):e4616.
- [3] Vasileiadis D, Drosos G, Charitoudis G, Dontas IA, Vlamis J. The efficacy of high-intensity preoperative physiotherapy training on postoperative outcomes in Greek patients undergoing total knee arthroplasty: a quasi-experimental study. *Cureus* 2022;14(3):e23191.
- [4] Palecek JJ. SMC5/6: multifunctional player in replication. *Genes* 2018;10(1).
- [5] Al-Modawi RN, Brinchmann JE, Karlsen TA. Multi-pathway protective effects of MicroRNAs on human chondrocytes in an in vitro model of osteoarthritis. *Mol Ther Nucleic Acids* 2019;17:776–90.
- [6] Fuggle NR, Cooper C, Oreffo ROC, Price AJ, Kaux JF, Maheu E, et al. Alternative and complementary therapies in osteoarthritis and cartilage repair. *Aging Clin Exp Res* 2020;32(4):547–60.
- [7] Sanchez-Lopez E, Coras R, Torres A, Lane NE, Guma M. Synovial inflammation in osteoarthritis progression. *Nat Rev Rheumatol* 2022;18(5):258–75.
- [8] Mariano A, Bigioni I, Misiti F, Fattorini L, Scotto D, Abusco A, et al. The nutraceuticals as modern key to achieve erythrocyte oxidative stress fighting in osteoarthritis. *Curr Issues Mol Biol* 2022;44(8):3481–95.
- [9] Wu CL, Harasymowicz NS, Klimak MA, Collins KH, Guilak F. The role of macrophages in osteoarthritis and cartilage repair. *Osteoarthritis Cartilage* 2020;28(5):544–54.
- [10] Zhang H, Cai D, Bai X. Macrophages regulate the progression of osteoarthritis. *Osteoarthritis Cartilage* 2020;28(5):555–61.
- [11] Yoshino H, Sato Y, Nakano M. KPNB1 inhibitor importazole reduces ionizing radiation-increased cell surface PD-L1 expression by modulating expression and nuclear import of IRF1. *Curr Issues Mol Biol* 2021;43(1):153–62.
- [12] Kidane D, Chae WJ, Czochoz J, Eckert KA, Glazer PM, Bothwell AL, et al. Interplay between DNA repair and inflammation, and the link to cancer. *Crit Rev Biochem Mol Biol* 2014;49(2):116–39.
- [13] Fujita T, Reis LF, Watanabe N, Kimura Y, Taniguchi T, Vilcek J. Induction of the transcription factor IRF-1 and interferon-beta mRNAs by cytokines and activators of second-messenger pathways. *Proc Natl Acad Sci U S A* 1989;86(24):9936–40.
- [14] Chen W, Zhang W, Zhou T, Cai J, Yu Z, Wu Z. A newly defined pyroptosis-related gene signature for the prognosis of bladder cancer. *Int J Gen Med* 2021;14:8109–20.
- [15] Karki R, Sharma BR, Lee E, Banoth B, Malireddi RKS, Samir P, et al. Interferon regulatory factor 1 regulates PANoptosis to prevent colorectal cancer. *JCI Insight* 2020;5(12).
- [16] Yang X, Liu H, Ye T, Duan C, Lv P, Wu X, et al. AhR activation attenuates calcium oxalate nephrocalcinosis by diminishing M1 macrophage polarization and promoting M2 macrophage polarization. *Theranostics* 2020;10(26):12011–25.
- [17] Masliah-Planchon J, Bièche I, Guinebretière JM, Bourdeaut F, Delattre O. SWI/SNF chromatin remodeling and human malignancies. *Annu Rev Pathol* 2015;10:145–71.
- [18] Sohn DH, Lee KY, Lee C, Oh J, Chung H, Jeon SH, et al. SRG3 interacts directly with the major components of the SWI/SNF chromatin remodeling complex and protects them from proteasomal degradation. *J Biol Chem* 2007;282(14):10614–24.
- [19] Jeong SM, Lee C, Lee SK, Kim J, Seong RH. The SWI/SNF chromatin-remodeling complex modulates peripheral T cell activation and proliferation by controlling AP-1 expression. *J Biol Chem* 2010;285(4):2340–50.
- [20] Lee SW, Park HJ, Jeon J, Park YH, Kim TC, Jeon SH, et al. Ubiquitous overexpression of chromatin remodeling factor SRG3 exacerbates atopic dermatitis in NC/nga mice by enhancing Th2 immune responses. *Int J Mol Sci* 2021;22(4).
- [21] Mankin HJ, Johnson ME, Lippiello L. Biochemical and metabolic abnormalities in articular cartilage from osteoarthritic human hips. III. Distribution and metabolism of amino sugar-containing macromolecules. *J Bone Joint Surg Am* 1981;63(1):131–9.
- [22] Abramoff B, Caldera FE. Osteoarthritis: pathology, diagnosis, and treatment options. *Med Clin North Am* 2020;104(2):293–311.
- [23] Hwang HS, Kim HA. Chondrocyte apoptosis in the pathogenesis of osteoarthritis. *Int J Mol Sci* 2015;16(11):26035–54.
- [24] Takács-Buia L, Iordachel C, Efimov N, Caloianu M, Montreuil J, Bratosin D. Pathogenesis of osteoarthritis: chondrocyte replicative senescence or apoptosis? *Cytometry B Clin Cytom* 2008;74(6):356–62.
- [25] Sun XH, Liu Y, Han Y, Wang J. Expression and significance of high-mobility group protein B1 (HMGB1) and the receptor for advanced glycation end-product (RAGE) in knee osteoarthritis. *Med Sci Monit* 2016;22:2105–12.
- [26] Ho YJ, Lu JW, Ho LJ, Lai JH, Huang HS, Lee CC, et al. Anti-inflammatory and anti-osteoarthritis effects of Cm-02 and Ck-02. *Biochem Biophys Res Commun* 2019;517(1):155–63.
- [27] Liu J, Cao L, Gao X, Chen Z, Guo S, He Z, et al. Ghrelin prevents articular cartilage matrix destruction in human chondrocytes. *Biomed Pharmacother* 2018;98:651–5.
- [28] Griffin TM, Scanzello CR. Innate inflammation and synovial macrophages in osteoarthritis pathophysiology. *Clin Exp Rheumatol* 2019;37(5):57–63. Suppl 120.
- [29] Hey J, Paulsen M, Toth R, Weichenhan D, Butz S, Schatterny J, et al. Epigenetic reprogramming of airway macrophages promotes polarization and inflammation in muco-obstructive lung disease. *Nat Commun* 2021;12(1):6520.
- [30] Zhong Z, Liang S, Sanchez-Lopez E, He F, Shalpour S, Lin XJ, et al. New mitochondrial DNA synthesis enables NLRP3 inflammasome activation. *Nature* 2018;560(7717):198–203.
- [31] Zafar A, Pong Ng H, Diamond-Zaluski R, Kim GD, Ricky Chan E, Dunwoodie SL, et al. CITED2 inhibits STAT1-IRF1 signaling and atherogenesis. *Faseb j* 2021;35(9):e21833.
- [32] Lee SW, Park HJ, Jeon J, Park YH, Kim TC, Jeon SH, et al. Chromatin regulator SRG3 overexpression protects against LPS/D-GalN-induced sepsis by increasing IL10-producing macrophages and decreasing ifn γ -producing NK cells in the liver. *Int J Mol Sci* 2021;22(6).
- [33] Lee SW, Park HJ, Jeon SH, Lee C, Seong RH, Park SH, et al. Ubiquitous overexpression of chromatin remodeling factor SRG3 ameliorates the T cell-mediated exacerbation of EAE by modulating the phenotypes of both dendritic cells and macrophages. *PLoS One* 2015;10(7):e0132329.
- [34] Ayyappan V, Sripathi VR, Kalavacharla VK, Saha MC, Thimmapuram J, Bhide KP, et al. Genome-wide identification of histone methylation (H3K9(me2)) and acetylation (H4K12(ac)) marks in two ecotypes of switchgrass (*Panicum virgatum* L.). *BMC Genom* 2019;20(1):667.
- [35] Cai Z, Long T, Zhao Y, Lin R, Wang Y. Epigenetic regulation in knee osteoarthritis. *Front Genet* 2022;13:942982.
- [36] Gagliano SA, Pouget JG, Hardy J, Knight J, Barnes MR, Ryten M, et al. Genomics implicates adaptive and innate immunity in Alzheimer's and Parkinson's diseases. *Ann Clin Transl Neurol* 2016;3(12):924–33.
- [37] Haque ME, Jakaria M, Akther M, Cho DY, Kim IS, Choi DK. The GCN5: its biological functions and therapeutic potentials. *Clin Sci (Lond)* 2021;135(1):231–57.
- [38] Mutlu B, Puigserver P. GCN5 acetyltransferase in cellular energetic and metabolic processes. *Biochim Biophys Acta Gene Regul Mech* 2021;1864(2):194626.
- [39] Lu M, Zhao B, Liu M, Wu L, Li Y, Zhai Y, et al. Pan-cancer analysis of SETD2 mutation and its association with the efficacy of immunotherapy. *npj Precis Oncol* 2021;5(1):51.